

# Modeling and experimental investigation of cantilever dynamics in force detected single electron tunneling

Levente J. Klein<sup>a)</sup> and Clayton C. Williams<sup>b)</sup>

*Department of Physics, University of Utah, Salt Lake City, Utah 84112*

(Received 4 September 2003; accepted 24 November 2003)

The dynamic response of a voltage biased oscillating cantilever probe is investigated through experimental and theoretical analysis as it approaches a dielectric surface. When the tip reaches the appropriate gap single electron tunneling events are detected between the metallic tip and the surface. The tunneling events cause a decrease of the electrostatic force and force gradient acting between tip and sample. The change in the electrostatic force is detected as an abrupt decrease of the cantilever oscillation amplitude. Additionally, due to the nonlinear interaction between tip and sample, the cantilever oscillation amplitude in very close proximity of the sample can have multiple values. Typically, as the tip-sample gap is reduced, a transition between two stable cantilever oscillation modes is detected as an abrupt increase in the oscillation amplitude. If this transition occurs at a gap larger than the tunneling gap, no tunneling event is detected. A theoretical model that includes both the electrostatic and mechanical effects has been developed to investigate the cantilever response in close proximity of the sample. The model, which includes the effects of the single electron tunneling events, is in good agreement with the measurements. © 2004 American Institute of Physics. [DOI: 10.1063/1.1641519]

## I. INTRODUCTION

Electrostatic force microscopy (EFM) has been used to investigate the time evolution of charge transferred from a metallic tip to insulator surfaces by contact charging<sup>1</sup> or corona discharge.<sup>2</sup> While in these early experiments the total amount of charge transferred to the surface was hard to control, single electron sensitivity to charge decay was demonstrated.<sup>2</sup> In addition, trapped holes in SiO<sub>2</sub> thin dielectric films<sup>3</sup> and atomic defects on GaAs surfaces<sup>4</sup> have been imaged with high spatial resolution by EFM. In all these methods the high sensitivity of the EFM to detect surface potential variations has been used to probe the presence of charge near the surface. Only recently has it been shown that single electron tunneling events can be detected between a metallic probe and insulator surfaces.<sup>5</sup> The method is based on measuring the electrostatic force variation between the scanning probe tip and the isolating surface.

To prove that electron tunneling can be detected by measuring electrostatic force<sup>6,7</sup> a special scanning probe was fabricated with an isolated metallic dot (200 nm in diameter) at the end of an oxidized cantilever. The metallic dot acts like a floating electrode. Addition or subtraction of a single charge changes the potential of the dot and the electrostatic force acting on the tip. The cantilever with the isolated metallic dot at its end is positioned 50 nm above the sample and then moved to the tunneling gap from the surface for a very short period of time. At the tunneling gap ( $\sim 1.5$  nm) the probability for electrons to tunnel from the tip to the surface has a finite value. The electrostatic force signals before and after

the cantilever movement are recorded. If no tunneling occurs, no change in the EFM amplitude signal is detected before and after the cantilever movement. If electrons tunnel to the surface, the electrostatic force signal shows a detectable change in magnitude before and after it is moved within tunneling range.

Another way to approach the sample to within the tunneling gap is to use the resonance response of the oscillating cantilever. By driving the cantilever at a fixed frequency below resonance, as the tip sample gap is reduced, the increased force gradient shifts the natural resonance frequency toward the drive frequency. The amplitude increases as the resonance frequency shifts toward lower values and the tip-sample gap is reduced until the cantilever reaches the tunneling gap. When the tip comes into tunneling range (tunneling probability is finite) an electron tunnels from the tip to the surface and the oscillation amplitude is reduced (increasing the gap). To detect another tunneling event the gap must be further reduced until the tip enters the tunneling range again. Many consecutive single electron tunneling events were observed in this way.<sup>7</sup>

Since single electron charging/discharging of an isolated metallic dot at the end of an atomic force microscopy (AFM) cantilever can be measured with high signal to noise ratio, the same techniques can be used to detect tunneling to localized electron states on insulator surfaces. In this approach a commercial metal coated AFM cantilever is used. The localized states on the insulator surface (spatially confined states with very long electron lifetimes) act as the isolated metallic dot at the end of the fabricated probes.<sup>5</sup> By recording simultaneously the optical deflection signal and the amplitude of the oscillating cantilever, it has been shown that no contact is made between the tip and surface when tunneling occurs. As the tip approaches the sample surface the cantilever oscilla-

<sup>a)</sup>Present address: University of Wisconsin, Madison, WI 53706.

<sup>b)</sup>Author to whom correspondence should be addressed; electronic mail: clayton@physics.utah.edu

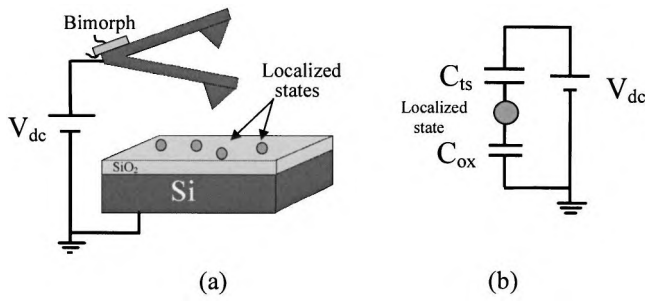


FIG. 1. Experimental setup (a), and the equivalent electric circuit (b) for electrostatic force detected tunneling experiment. A voltage ( $V_{dc}$ ) biased probe approaches the surface to tunneling range where  $C_{ts}$  is the tip-sample capacitor in series with the oxide capacitance ( $C_{ox}$ ).

tion becomes nonlinear and the gap where the tunneling events occur is very close to the gap where the oscillating cantilever encounters a mechanical instability. In the proximity of the sample, the cantilever can have more than one allowed oscillation mode. The instability occurs when the cantilever oscillation jumps between the different oscillation modes. In order to separate the electron tunneling events from the mechanical instability of the cantilever, a theoretical model is developed in this article that describes the cantilever motion in the proximity of the sample. Similar instabilities have been detected and modeled previously under different experimental conditions by other groups,<sup>8–10</sup> however, no clear understanding and description exists about the physical origin of the jump between the oscillation modes. In the model proposed in this article, it is assumed that during each cycle of oscillation the cantilever senses a nonlinear electrostatic force acting between tip and sample. Far from the surface the resonance curve is Lorentzian in shape, but as the tip-sample gap is reduced it becomes distorted and more than one amplitude is possible at a given frequency. The resonance curve is composed of two branches. The model proposed in this article explains the instability observed in the amplitude as being due to the jump of the oscillation from one branch of the resonance curve to another at a given gap. Comparing experimental data with the simulations shows good agreement. The proposed model is useful for exploring the experimental conditions where tunneling events can be separated from the instability. If the instability occurs at a larger tip-sample gap than the tunneling gap, it can make the observation of electron tunneling events impossible.

## II. TIP-SAMPLE INTERACTION MODELING

### A. Electrostatic force

In Fig. 1 the experimental setup and the corresponding equivalent circuit are shown for a voltage biased metallic cantilever oscillated above an insulating layer on a Si substrate. A capacitance is formed between the end of the cantilever and surface ( $C_{ts}$ ). This capacitance is in series with the oxide (insulating layer) capacitance ( $C_{ox}$ ). The two capacitances in series,  $C_{ts}$  and  $C_{ox}$ , act as a voltage divider and the voltage between tip and sample surface is

$$V_{ts} = \frac{V_{dc} C_{ox}}{C_{ox} + C_{ts}}. \quad (1)$$

At a large tip-sample gap almost the entire applied dc voltage drops between the tip and oxide surface while at a smaller tip-sample gap just a fraction of the total voltage will drop between the tip and sample surface. For example, in the measurements presented in this article, the dc voltage applied to the sample is 5 V, and for an oxide thickness of 20 nm and a tunneling gap of 1.5 nm, the voltage drop between the tip and sample surface is 1.5 V.

To simplify the calculations a parallel plate approximation is assumed where the capacitance is inversely proportional to the gap. The electrostatic force acting on the tip is

$$F = \frac{C_{ts} C_{ox}^2}{(C_{ts} + C_{ox})^2} \frac{V_{dc}^2}{2z} = \frac{C_{ts} V_{dc}^2}{2} \frac{z}{\left(z + \frac{z_{ox}}{\epsilon_{ox}}\right)^2}, \quad (2)$$

where  $z$  is the tip-sample gap,  $z_{ox}$  is the oxide thickness, and  $\epsilon_{ox}$  is the dielectric constant of the oxide film. As the tip approaches the sample, the increased force gradient shifts the resonance frequency to a lower value. The force gradient sensed by the cantilever is

$$F'_{dc} = \frac{C_{ts} C_{ox}^3}{(C_{ts} + C_{ox})^3} \frac{V_{dc}^2}{z^2}. \quad (3)$$

In the case of a very large oxide capacitance ( $C_{ox} \gg C_{ts}$ ), the force gradient becomes the well known expression for a parallel plate capacitor.

### B. Modeling the tunneling

With a negative voltage applied to the tip, with respect to the sample, electrons are most likely to tunnel from tip to surface. The oxide film is assumed to be a thin dielectric layer that has localized electronic states with long lifetimes distributed on the surface. The existence and distribution of charge states on/in  $\text{SiO}_2$  films have been measured previously.<sup>3</sup> For modeling purposes, it is assumed that a given localized state is below the apex of the tip, with an energy level in the band gap of the oxide film. Such a state is weakly coupled to the conduction/valence band and other nearby surface states, giving it a long lifetime. It is assumed that if an electron tunnels to such a state, it will stay localized and the probability of tunneling/hopping to other states is negligible.

Figure 2 shows the electrostatic force variation due to an electron tunneling to the insulator surface. Before tunneling, the force sensed by the cantilever is proportional to the density of field lines that terminate on the tip. If an electron tunnels to the surface, some of the field lines will end on the electron and the field line density will be decreased on the tip. This will cause a decrease in the force and force gradient sensed by the cantilever. The same reasoning is valid if the voltage applied to the sample is reversed in sign (positive voltage on the tip). In this case an electron will likely tunnel from the surface to the tip, leaving a positive charge on the surface. In both cases the voltage drop between tip and

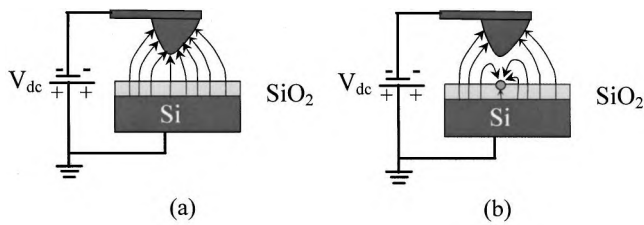


FIG. 2. (a) Electric field lines between a metallic tip and a thin dielectric (SiO<sub>2</sub>) covered Si substrate before (a) and after (b) an electron tunneling event. After tunneling the electrostatic force sensed by the cantilever decreases.

sample surface decreases as an electron tunnels to or from the surface, causing a decrease in the force gradient.

Using the equivalent circuit in Fig. 1, in the parallel plate approximation, the surface state is modeled as a floating metallic plate between the conducting electrodes of the tip/sample capacitor. If electron tunneling occurs to/from the isolated state, the voltage between the tip and sample decreases as

$$|V_{ts}| = \frac{|V_{dc}|C_{ox} - |q|}{C_{ox} + C_{ts}}, \quad (4)$$

where  $q$  is the magnitude of charge that tunnels (for a single electron case  $q = +1.6 \times 10^{-19}$  C). The electrostatic force gradient is

$$F'_{dc} = \frac{C_{ts}C_{ox}^3}{(C_{ts} + C_{ox})^3} \frac{\left(|V_{dc}| - \frac{|q|}{C_{ox}}\right)^2}{z^2}, \quad (5)$$

which is similar to the case where no electron tunneling is included, except for an adjustment of the applied dc voltage. The variation of the force gradient due to tunneling is proportional to the amount of charge that tunneled. If the sign of the voltage applied to the sample is reversed, the same dependence of force gradient on charge is obtained.

### III. EXPERIMENTAL MEASUREMENTS

The experiments are performed in high vacuum ( $10^{-9}$  Torr) using commercial Pt coated cantilevers. The samples are high quality thermally grown 20-nm-thick SiO<sub>2</sub> films grown on silicon substrates. The characteristics of the cantilevers used in these experiments are: resonance frequency 230 kHz, quality factor 30 000, and nominal spring constant 40 N/m. The samples were heated to 600 °C for half an hour before the measurements. The surface is approached in contact mode. Once contact is made the feedback loop is disengaged and the cantilever is lifted 100 nm above the surface. The cantilever is oscillated at a couple of thousand hertz below its natural resonance frequency by applying an ac voltage to the piezoelectric bimorph attached to the back of the cantilever. Both amplitude and phase of the oscillating cantilevers is detected using a lock-in amplifier. A dc voltage is applied to the sample with respect the tip potential (typically  $\pm 2-5$  V relative to the flatband). The cantilever is brought close to the surface by applying an offset voltage to the piezotube attached to the sample. As the cantilever

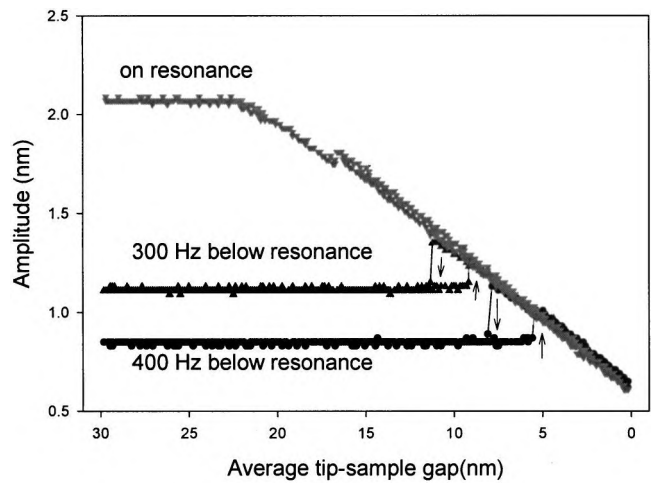


FIG. 3. Instability detected in the oscillation amplitude of a cantilever driven on resonance, 300 and 400 Hz below resonance. The arrows indicate the cantilever direction of motion.

approaches the sample, the increased force gradient shifts (due to the electrostatic force) the natural resonance frequency toward lower values. The resonance frequency shift causes an increase of the oscillation amplitude of the cantilever. To achieve the highest sensitivity for EFM measurements, the drive frequency is chosen such that at the tunneling gap the resonance frequency is almost equal to the drive frequency.

The oscillating cantilever is pushed toward the surface until contact is made. As the oscillating tip approaches the sample surface, a gradual increase of the amplitude is detected followed by an abrupt increase in amplitude very close to the sample surface. The abrupt changes are observed both in amplitude and phase. The jump is due to a transition between two possible oscillation modes of the cantilever in close proximity of the sample. In our experiment it has been observed that the gap where the jump occurs (amplitude and phase) is determined in part by the drive frequency value and by the oscillation amplitude of the cantilever. The gap where the instability occurs is reduced if the cantilever is driven farther away from the resonance frequency or the drive amplitude of the cantilever oscillation is decreased. Figure 3 shows the oscillation amplitude for a case when the oscillation drive amplitude is kept constant but the drive frequency is shifted away from resonance. The jumps occur closer to the surface as the drive frequency is decreased with respect to the resonance frequency. As the difference between the drive and resonance frequency increases a hysteresis in amplitude where the jumps occur is observed. The cantilever direction of motion is marked on the graph. The gap where the jump (increase in amplitude) occurs as the tip approaches the sample is smaller than the gap where the jump occurs (decrease in amplitude) as the tip retracts. To observe tunneling events, the gap where the increase occurs between the two stable solutions should be smaller than the tunneling gap ( $\sim 1.5$  nm). To achieve this regime, with a large voltage applied between the tip and the sample, the cantilever has to be

driven a few thousand hertz below the natural resonance frequency.

To detect electron tunneling events between an AFM tip and sample, the oscillating cantilever tip must reach the tunneling range to the surface. In general, before the instability occurs, the electron tunneling probability between the tip and the states of the surface has an exponential dependence on the gap. There are two characteristic distances associated with the tip-sample gap. One is the average tip-sample gap and the other is the minimum tip sample gap (different due to the oscillation of the cantilever). Because of the exponential dependence upon the gap, tunneling will most likely occur at the minimum tip sample gap (the smallest distance between the apex of the tip and the sample surface). In order to detect tunneling from the AFM tip to an insulator surface, two conditions should be fulfilled at the same time. Empty states should exist on the surface of the insulator near the tip and the tunneling probability must have a finite value. Far from the surface the tunneling probability is negligible on the time scale of the experiment. By reducing the average (and thus minimum) tip sample gap, the tunneling probability increases exponentially. As the tip-sample gap approaches the tunneling range, the most statistically probable event is that a single electron tunnels. The tunneling of more than one electron (double event) is less likely. Once an electron tunnels, the amplitude of the cantilever oscillation is decreased (the minimum gap is increased and the tunneling probability becomes small again) and no other tunneling can occur until the minimum gap is further reduced to the tunneling range, making the tunneling probability finite again.

During tunneling experiments, the oscillating cantilever is moved toward the sample surface above different locations on the sample. In most of the cases, no tunneling is observed. That may be due to the absence of empty surface states to which an electron can tunnel. By further approaching the sample the jump in amplitude (instability) is detected. Once the cantilever jumps to the second oscillation mode, the EFM sensitivity (minimum detectable surface potential variation) is highly reduced.

Typically there are locations on the  $\text{SiO}_2$  surface where tunneling does occur, and in this case, a small decrease in amplitude is detected before the instability in the amplitude is encountered. Since electron tunneling decreases the electrostatic force and force gradient sensed by the cantilever, the tunneling events can be distinguished from the instability observed. Electron tunneling abruptly reduces the amplitude, while the instability abruptly increases the amplitude. When tunneling is detected most of the events are single electron tunneling events

Figure 4 shows the amplitude response of the cantilever as it approaches the surface. No tunneling is detected in the first case [Fig. 4(a)], however, an abrupt increase (instability) in amplitude is observed. Figure 4(b) shows a single electron tunneling event as the cantilever approaches the surface. The tunneling event causes a decrease in the amplitude of oscillation. Since the minimum gap increases (by 0.02 nm) just after tunneling (tunneling probability decreases) no other electron tunnels until the gap is further reduced. With further

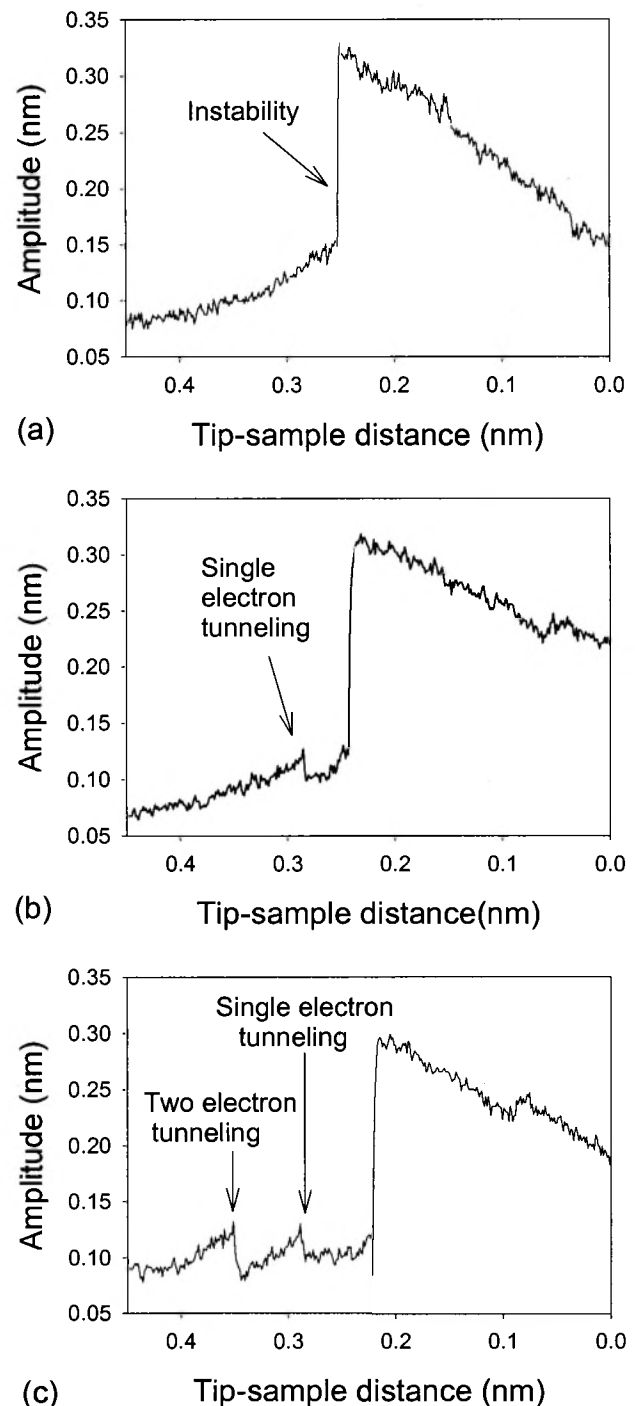


FIG. 4. (a) Instability of the cantilever with no electron tunneling event, (b) single electron tunneling, and (c) two electron tunneling followed by a single electron tunneling.

movement toward the sample, the instability in amplitude is ultimately detected.

There are locations on the surface where more than one electron can tunnel to the surface. These locations may correspond to extended defects which can accommodate more than one electron. Every time the tip comes within tunneling range, a new tunneling event may occur. In Fig. 4(c) consecutive tunneling events are detected as the cantilever moves toward the surface. Some of the tunneling events produce amplitude variations twice as large as others. Occasion-

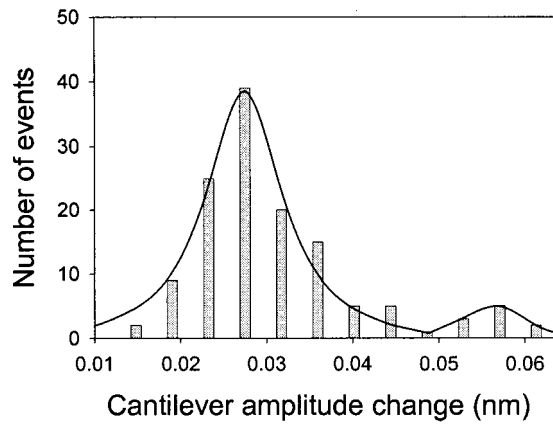


FIG. 5. Histogram of amplitude variation for 131 tunneling events.

ally, if two electrons tunnel at the same time, the amplitude variation can be almost twice as large as that due to a single electron tunneling event. As can be observed in Fig. 4(c), the amplitude change for the first event is approximately twice as large as for the next tunneling event. During the first tunneling event two electrons tunnel at the same time followed by another event corresponding to a single electron tunneling event. Two electrons tunneling at the same time is possible since occasionally there may be two empty states on the surface at equal distance from the apex of the tip.

After observing many tunneling events, a histogram of the events was generated. The amplitude change for 131 tunneling events was analyzed and the variation in amplitude is plotted in Fig. 5. The data were taken at many different locations on the surface, at both positive and negative bias. A bin size of 0.005 nm is used. The histogram shows a peak centered on 0.028 nm corresponding to tunneling events produced by single electrons. There is a small second peak around 0.057 nm, which is almost twice the magnitude of the first. This peak corresponds to two simultaneous tunneling events as observed previously. Since the electron charge is quantized, if the peak at 0.028 nm corresponded to more than one event, other peaks would be expected at lower amplitude value corresponding to single electron tunneling event.

The width of the peaks in the histogram can be due to several different sources. First, the local surface potential variation on the surface may cause variation in the event amplitude. Also the states to which the electrons tunnel may be located just below the dielectric surface or off the tip apex. In such circumstances, the tip must approach the sample to a smaller gap so that tunneling can take place, changing the event amplitude. These effects broaden the histogram peaks.

The ability to detect single electron tunneling to localized states on insulator surfaces allows one to electrically characterize insulator surfaces. By scanning an insulator surface, the location of surface states can be detected as the places where single electron tunneling takes place. Once the locations of the surface states are found, an electronic spectroscopy can be performed on these surface states: the tip sample gap is kept constant and the voltage applied to the tip is ramped until an electron tunneling event is detected. If the voltage at which electron tunneling to the surface is known,

the energy of the surface states can be calculated. Since scanning tunneling microscopy has atomic scale spatial resolution,<sup>11</sup> it is expected that single electron tunneling will also provide atomic scale spatial resolution. To characterize insulating surfaces with single electrons, the tip sample gap should be controlled with high precision and the cantilever behavior in the proximity of the sample should be thoroughly understood, including the mechanical instability.

#### IV. FORCE DETECTED ELECTRON TUNNELING SIMULATION

##### A. Small amplitude approximation

The mechanical response of the cantilever to single electron tunneling events between the probe and surface has been simulated using the small amplitude approximation. In the small amplitude approximation, the cantilever oscillation amplitude is assumed much smaller than the average tip-sample gap and the force gradient sensed by the cantilever depends only on the average tip-sample gap. In this approximation, the amplitude  $A$  and phase  $\varphi$  of the oscillating cantilever can be expressed as<sup>12</sup>

$$A = \frac{a}{\sqrt{\left(1 - \frac{\omega^2}{\omega_0^2} - \frac{F'_{dc}}{k_0}\right)^2 + \frac{\omega^2}{Q^2\omega_0^2}}},$$

$$\sin(\varphi) = \frac{\omega}{\omega_0} \frac{A}{Qa}, \tag{6}$$

where  $a$  is the mechanical drive amplitude of the cantilever,  $k_0$  is the spring constant,  $\omega$  is the drive frequency,  $\omega_0$  is the natural resonance frequency (far from surface),  $Q$  is the quality factor of the cantilever, and  $F'_{dc}$  is the force gradient.

The tunneling is included in this model by using a force gradient (formula 5) which is dependent on the charge on the surface, by changing the value of  $q$  from zero to one electron when the cantilever is at 1.56 nm from the surface. The 1.56 nm gap is determined from a tunneling calculation and corresponds to the tip-sample gap where an electron would tunnel to a localized state in an average time of 1 s. To compare the simulations with experimental data, a data set of amplitude and optical deflection signal of the oscillating cantilever is acquired, including a single electron tunneling event and the instability. The optical deflection signal shows that when the tunneling occurs no contact is made between the tip and the sample.<sup>5</sup> The parameters used in the simulations are: quality factor  $Q = 30\,000$ , spring constant 40 N/m, resonance frequency 328 kHz, drive frequency 4.5 kHz below resonance, oxide thickness 20 nm, and the dc voltage applied to the sample is 5 V. Single electron tunneling is assumed for this simulation, however, the model can be modified to include consecutive tunneling events whenever the tip is within the tunneling range of the surface. Figure 6 shows an experimental trace of the amplitude variations including a single electron tunneling event along with a curve obtained with the small amplitude simulations. A good agreement is obtained, including the tunneling event (abrupt drop in amplitude) for the cantilever response up until the mechanical

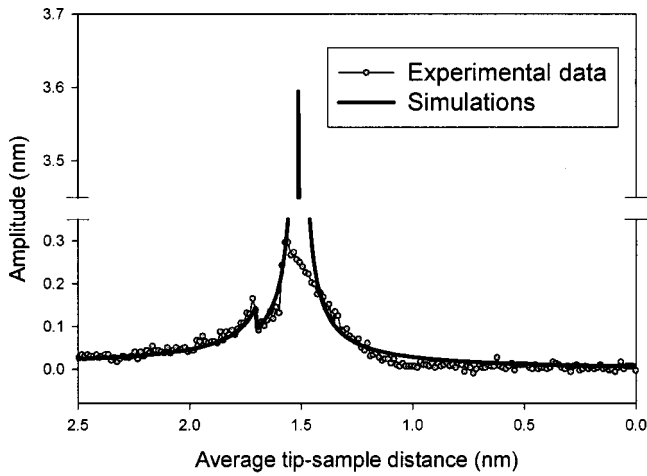


FIG. 6. Overlap of experimental data and simulation of a single electron tunneling event using the small amplitude approximation model.

instability occurs. The radius of the tip was the adjusted parameter to fit the experimental data. For this simulation the tip radius was assumed to be 35 nm which is in the proper parameter range of the probes used. The simulation cannot predict the instability encountered by the cantilever, detected as the abrupt increase in amplitude following the tunneling event. In the small amplitude approximation model the resonance curve is Lorentzian in shape and has a single amplitude value for any given frequency. Even so, the small approximation model can be applied to describe the tunneling event since the oscillation amplitude of the cantilever at that gap is much smaller than the average tip-sample gap, as shown in Fig. 6.

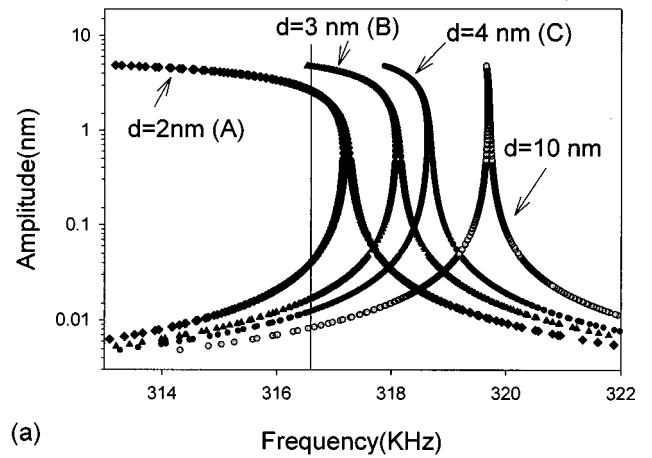
### B. Nonlinear tip-sample interaction

An extension of the small amplitude approximation model would be to consider the nonlinear tip sample interaction. To calculate the amplitude and phase of the cantilever, the differential equation that describes the cantilever motion should be solved. It is assumed that the force acting between the tip and the sample is modulated by the cantilever motion. During each cycle of the oscillation a larger force will be sensed by the cantilever when it is closest to the surface and a smaller magnitude when it is further away from the surface. The force gradient will increase as the average tip-sample gap is decreased.

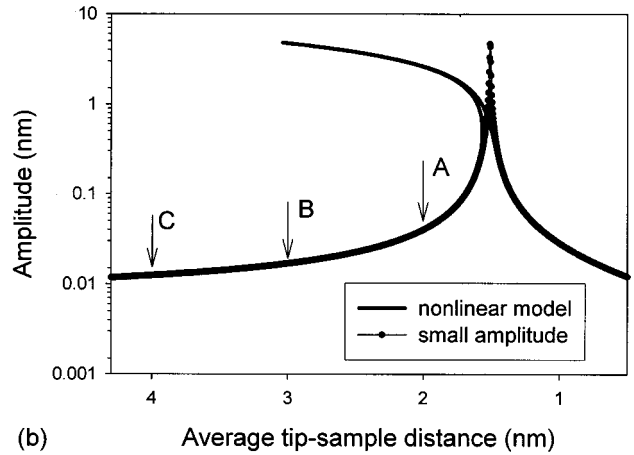
The differential equation that describes the cantilever motion is

$$\ddot{Z} + \omega_0^2 Z + \frac{\omega_0}{Q} \dot{Z} = \frac{\omega_0^2}{k_0} F, \tag{7}$$

where  $Z$  is the position measured from the surface and  $F$  is the force sensed by the tip. For a periodically driven cantilever, the force is  $F = k_0 a \cos(\omega t) + F(\omega)$ , where  $k_0$  is cantilever spring constant and  $a \cos(\omega t)$  is the displacement at the back of the cantilever (driven by a piezoelectric bimorph).  $F(\omega)$  is the steady state periodic electrostatic force sensed by the cantilever due to the applied dc voltage between tip and sample and its harmonic motion.



(a)



(b)

FIG. 7. (a) Resonance curve distortion at different average tip-sample gaps predicted by the nonlinear model (b) comparison of the amplitude variation for the small amplitude and nonlinear model approximation as the tip approaches the sample. In (b) the gaps are marked where the resonance curves are plotted.

To solve this equation, the cantilever motion is assumed sinusoidal, described by  $Z = z + A \cos(\omega t + \varphi)$ , where  $z$  is the average tip-sample gap,  $A$  is the amplitude, and  $\varphi$  is the phase of oscillation of the cantilever. A sinusoidal motion of the cantilever in the proximity of the sample is in agreement with experimental data that analyzed the power spectrum density of the cantilever in the close proximity of the sample.<sup>13</sup>

The electrostatic force acting between the tip and sample with a cantilever oscillation is

$$F(\omega) = \frac{C_{ts} V_{dc}^2}{2} \frac{z}{\left[ z + \frac{z_{ox}}{\epsilon_{ox}} - A \cos(\omega t + \varphi) \right]^2}, \tag{8}$$

where  $A$  is the oscillation amplitude of the cantilever,  $z_{ox}$  and  $\epsilon_{ox}$  is the oxide thickness and dielectric constant, and  $V_{dc}$  is the applied dc voltage between the tip and sample.

Far from the surface ( $z \gg A$ ) the electrostatic force is approximately sinusoidal, but when the tip-sample gap is reduced, the force becomes nonsinusoidal. The cantilever will

sense a very large force and force gradient when the oscillation reduces the gap to a small value, due to the nonlinear dependence of the force on gap.

To solve the differential equation, the electrostatic force is Fourier decomposed in to its frequency components

$$\begin{aligned}
 F(\omega) &= a_0 + a_1 \sin(\omega t) + b_1 \cos(\omega t) + \dots, \\
 a_0 &= \frac{1}{T} \int_0^T F(\omega) dt, \\
 a_1 &= \frac{2}{T} \int_0^T F(\omega) \sin(\omega t) dt, \\
 b_1 &= \frac{2}{T} \int_0^T F(\omega) \cos(\omega t) dt. \tag{9}
 \end{aligned}$$

Because of the high  $Q$  of the system, only the dc term and the terms at the oscillation frequency ( $\omega$ ) need to be considered, as other terms will not produce significant displacements.

Using the Fourier decomposed electrostatic force and the oscillatory displacement, two coupled equations for the tip motion are obtained. Both equations contain amplitude and phase but an analytical solution can be deduced where the amplitude and phase of the cantilever oscillation can be expressed independent of each other.

The amplitude and phase of the oscillating cantilever as function of drive amplitude and the average tip-sample gap are

$$\begin{aligned}
 A &= \frac{a}{\sqrt{\left\{ 1 - \frac{\omega^2}{\omega_0^2} - \frac{C_{ts} V_{dc}^2 z}{k_0 \left[ \left( z + \frac{z_{ox}}{\epsilon_{ox}} \right)^2 - A^2 \right]^{3/2}} \right\}^2 + \frac{\omega^2}{Q^2 \omega_0^2}}}, \\
 \sin(\varphi) &= \frac{\omega}{\omega_0} \frac{A}{Qa}, \tag{10}
 \end{aligned}$$

where  $A$  is the amplitude of oscillation and  $\varphi$  is the phase of the oscillating cantilever. The equation expressing  $A$  as a function of  $z$  can be solved using a computational program like MAPLE.

The nonlinear model reduces to the small amplitude model if the amplitude ( $A$ ) is small compared to the gap ( $z$ ). The force gradient under this assumption ( $z \gg A$ ) becomes

$$F'_{dc} = \frac{C_{ts} V_{dc}^2 z}{\left[ \left( z + \frac{z_{ox}}{\epsilon_{ox}} \right)^2 - A^2 \right]^{3/2}} \approx \frac{C_{ts} C_{ox}^3}{(C_{ox} + C_{ts})^3} \frac{V_{dc}^2}{z^2}, \tag{11}$$

which is the force gradient obtained previously in the small amplitude model (formula 3). Also the amplitude [Eq. (10)] reduces to the amplitude of small approximation model.

The resonance frequency variation as a function of the average tip-sample gap is given by

$$\frac{\omega}{\omega_0} = \sqrt{\frac{(aQ)^2}{A^2} - \left\{ \frac{1}{2Q} \pm \sqrt{\frac{1}{4Q^2} - \left( 1 - \frac{(aQ)^2}{A^2} \right)} + \frac{C_{ts} V_{dc}^2 z}{k_0 \left[ \left( z + \frac{z_{ox}}{\epsilon_{ox}} \right)^2 - A^2 \right]^{3/2}} \right\}^2}. \tag{12}$$

Similar formulas were obtained by other groups using energy conservation principles<sup>8</sup> or a variational method.<sup>9</sup>

It can be observed that two frequency solutions are possible for a certain gap ( $z$ ) determined by the  $\pm$  sign in the front of the last square root term in Eq. (12) The resonance curve is composed of two branches: the left branch describes the cantilever behavior below resonance (+ sign) and the right branch above resonance and a finite range below resonance (- sign).

The nonlinear model predicts that when the cantilever is far from the surface the resonance curve is Lorentzian in shape. As the tip-sample gap is reduced the resonance curves become distorted. As the gap is further reduced the two branches become more distorted in shape and shift toward lower frequencies. A plot of the resonance curve distortion at different tip-sample gaps is shown in Fig. 7(a). The distortion in the resonance curves can be re-plotted as the amplitude variation versus gap change [Fig. 7(b)]. For comparison the amplitude versus gap variation for the small amplitude approximation is plotted in the same graph. Far from the sur-

face the two models agree well but as the gap is reduced the nonlinear model shows the multiple solution behavior. It is indicated in Fig. 7(b) the average gaps at which three different resonance curves were calculated. There is also a resonance curve plotted in Fig. 7(a) at a large tip sample gap (10 nm) where the resonance curve is approximately Lorentzian in shape. As the tip sample gap is reduced this Lorentzian curve gets distorted and shifted toward lower frequency values.

Experimentally, as the cantilever approaches the surface, the amplitude follows one of the branches of the resonance curve. In the tunneling experiments the cantilever is driven below the natural resonance frequency so it follows the left branch (lower solution) of the resonance curve. As the tip approaches the sample, the increased force gradient shifts the resonance frequency to lower values increasing the amplitude of oscillation. At a certain gap more than one amplitude solution becomes possible. The tip stays in the lower part of the left branch of the resonance curve. After further approach to the sample, a jump in amplitude is detected which is due

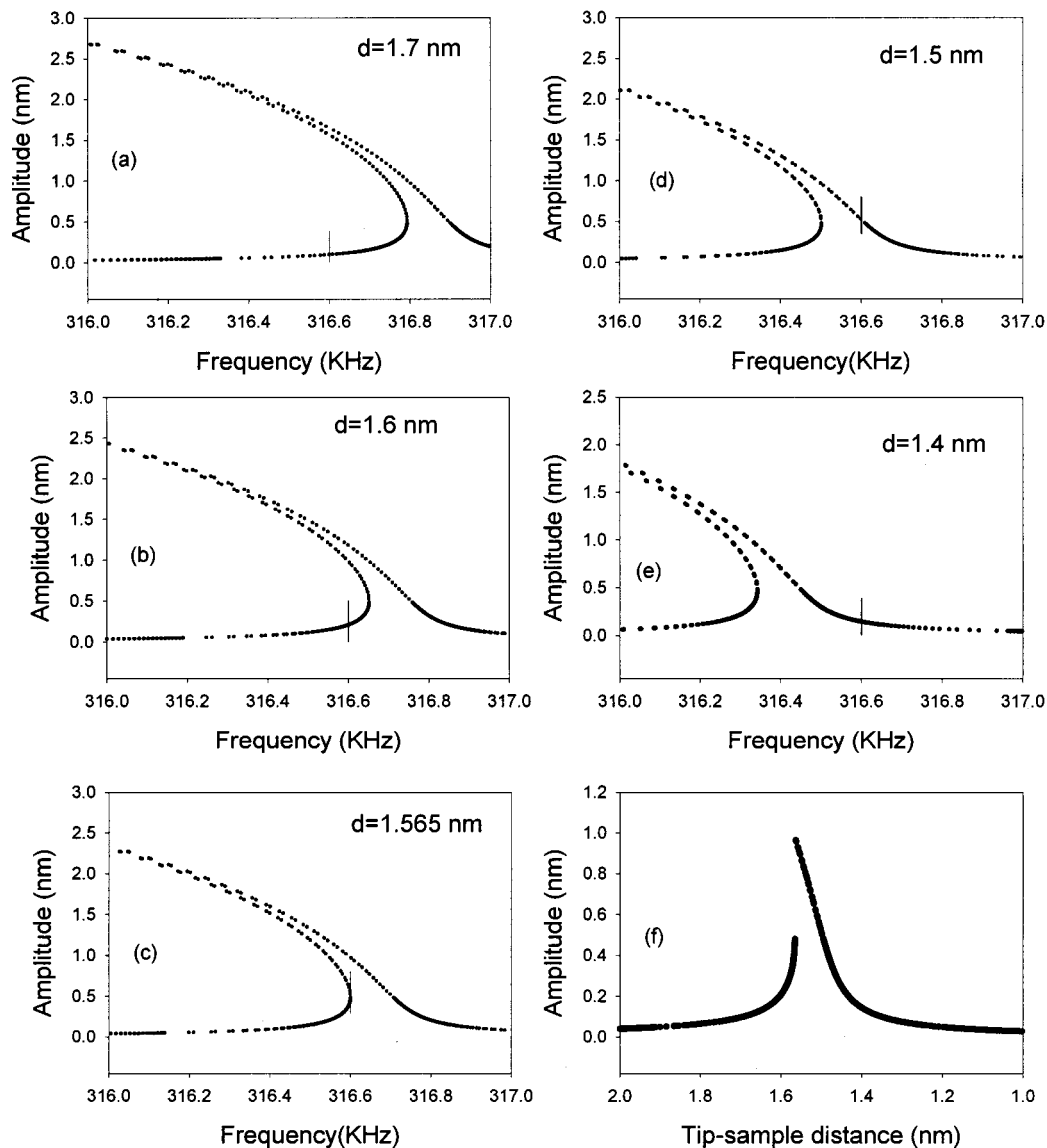


FIG. 8. Resonance curve distortion as the cantilever approaches the sample. For large tip-sample gaps the amplitude follows the left branch of the resonance curve [(a) and (b)] until a gap is reached (c) where no solution exists on the left branch for the working frequency (straight line). The oscillation then jumps to the right branch [(d) and (e)]. In (f) the amplitude variation of the oscillating cantilever is shown as the tip approaches the sample.

to the transition from the left branch of the resonance curve to the right one.

The abrupt jump in the amplitude can be understood by the resonance curve shape and movement as the tip approaches the sample. In our experiments the drive frequency of the cantilever is fixed. As the tip approaches the sample, the increasing force gradient shifts the actual resonance frequency toward lower values. For every tip-sample gap there is a corresponding resonance curve. The more the tip approaches the sample, the more the resonance curve gets distorted and shifted toward lower frequencies.

There is a gap where the left branch of the resonance curve is shifted so much toward lower frequencies that no amplitude solution corresponds to the drive frequency. The jump occurs when this gap is reached. Beyond this point, the only solution available is the right branch. The amplitude at that gap and drive frequency jumps to a higher value.

Figure 8 shows several resonance curves (amplitude ver-

sus frequency) at different tip-sample gaps. As the tip sample gap is reduced, the amplitude follows the lower left branch and it increases in magnitude [Figs. 8(a), 8(b), 8(c)]. When it reaches the gap where the left branch has no solution (just at the turning point, Fig. 8(c)) it jumps to the right branch and follows this branch [Figs. 8(d), 8(e)]. As seen in the figure, when the amplitude jumps to the right branch an increase in the amplitude occurs. Further reducing the tip sample gap, the amplitude follows the right branch and the amplitude decreases as the tip sample gap is further reduced. Figure 8(f) shows the simulated amplitude of the oscillating cantilever as the tip approaches the sample, including the effects shown in Figs. 8(a)–8(e). The amplitude response of the oscillating cantilever as the tip-sample gap is reduced is in a qualitative agreement with the experimental observations. Due to the resonance curve distortion three possible solutions of the amplitude can correspond to a certain gap. This can be observed in Figs. 8(a)–8(c) when the cantilever os-

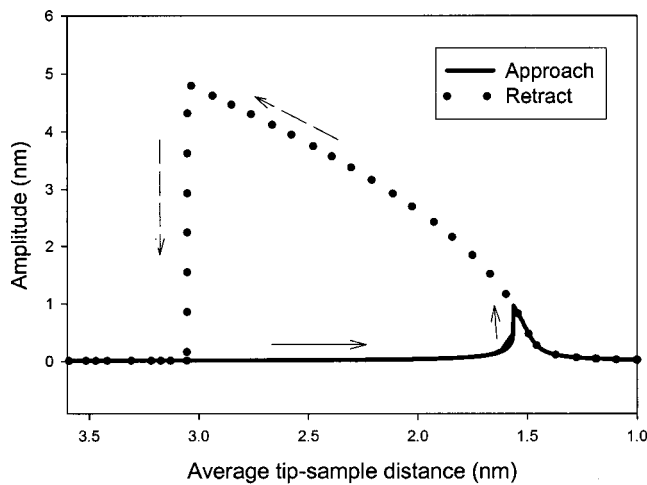


FIG. 9. Simulation of the amplitude hysteresis as the cantilever approaches and is retracted from the sample surface.

cillation follows the left branch (the drive frequency is marked by the straight line). It is observed experimentally that the upper branch of the left-hand solution, although mathematically possible is not reached.

The proposed model can explain also the hysteresis observed in amplitude where the instability occurs as the tip approaches/departs from the surface. As the tip sample gap is reduced the amplitude follows the lower left branch of the resonance curve until jumps to the right branch. Once on the right branch it will follow it down, as the tip sample gap is further reduced (until contact is made). When the tip is pulled back from the surface (gap is increased), the amplitude follows the right branch of the resonance curve until no possible right branch solution exists. The cantilever amplitude then drops to the lower left branch solution (abrupt change in amplitude) and follows it as the tip sample gap increases. Since the gap where the jump from the left to right branch occurs is smaller than the gap where the cantilever jumps from the right to the left branch, a hysteresis appears (Fig. 9). This is shown the experimental data in Fig. 3, where a hysteresis is observed when the drive frequency is below resonance.

Once the gap where the instability occurs is known, the simulated amplitude versus gap curve can be plotted taking into account the part of the amplitude curves that give a physical solution for the cantilever oscillations. When the minimum tip-sample gap reaches 1.56 nm a tunneling event is included in the simulation. The parameters in this simulation are exactly the same as for the previously described small amplitude approximation. The simulated amplitude variation for the nonlinear model including the tunneling event matches with experimental data as it is shown in Fig. 10. The tunneling event and the prediction of the gap where the jump is detected in amplitude is well predicted by the nonlinear model. The amplitude increase (magnitude) when the instability is encountered is still larger than the experimental data. In the proximity of the sample the quality factor of the cantilever is highly reduced and this may explain the different value of the amplitude when the instability occurs as predicted by the model and the experiment. In the simu-

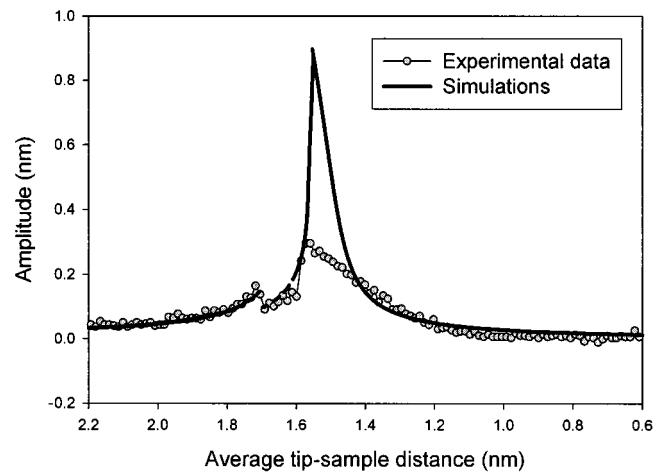


FIG. 10. Overlap of the experimental data for a single electron tunneling event and the nonlinear model simulation of the cantilever response. The nonlinear model predicts accurately the amplitude variation due to a single electron tunneling event and the gap where the cantilever encounters the instability.

lations the quality factor of the cantilever remains unchanged as the tip approaches the sample, until contact is made. The amplitude response of the cantilever over a large tip-sample gap is well simulated by the proposed theoretical model. The long range electrostatic force and force gradient sensed by the tip gives a good description of the tip-sample interactions. Taking into account the cantilever response predicted by the proposed theoretical model, the physical conditions can be explored under which single electron tunneling detection is possible. Separation of the gap where single electron tunneling events are detected from the gap where the cantilever encounters the instability should allow a stable scanning of the cantilever to map out localized surface states on the insulator surfaces.

## V. SUMMARY

Experimental evidence for single electron tunneling events from a metallic cantilever to an insulating surface is presented. The tunneling events occur in a region where the cantilever oscillation can encounter an instability. A theoretical model is presented that includes the electrostatic and mechanical effects on the oscillating cantilever. The model proposed describes accurately the cantilever behavior over a large tip sample gap including single electron tunneling events and the instability encountered by the oscillation. The instability in the amplitude detected as the oscillating cantilever approaches the sample is explained by the distortion of the resonance curve. Two branches of the resonance curve are identified and the instability in the amplitude detected experimentally are explained as a jump of the cantilever oscillation from one branch to the other. A good agreement is obtained between the experimentally measured single electron tunneling induced amplitude variation and the two models investigated in this article. The good fit of the experimental curves by the proposed theoretical models additionally supports that single electron tunneling event are measured between the tip and the sample. A good knowledge of the

cantilever behavior in the proximity of the sample should allow the separation of the tunneling events from the instability. The possibility of detecting single electron tunneling events between a metallic scanning probe tip and insulator surfaces opens the way to electrically characterizing insulator surfaces with atomic scale resolution.

<sup>1</sup>B. D. Terris, J. E. Stern, D. Rugar, and H. J. Mamin, Phys. Rev. Lett. **63**, 2669 (1989).

<sup>2</sup>C. Schoneberger and S. V. Alvarado, Phys. Rev. Lett. **65**, 3162 (1990).

<sup>3</sup>R. Ludeke and E. Cartier, Appl. Phys. Lett. **78**, 3998 (2001).

<sup>4</sup>Y. Sugawara, T. Uchihashi, M. Abe, and S. Morita, Appl. Surf. Sci. **140**, 371 (1999).

<sup>5</sup>L. J. Klein and C. C. Williams, Appl. Phys. Lett. **81**, 4589 (2002).

<sup>6</sup>L. J. Klein, C. C. Williams, and J. Kim, Appl. Phys. Lett. **77**, 3615 (2000).

<sup>7</sup>L. J. Klein and C. C. Williams, Appl. Phys. Lett. **79**, 1828 (2001).

<sup>8</sup>R. Garcia and R. Perez., Surf. Sci. Rep. **47**, 197 (2002).

<sup>9</sup>G. Couturier, L. Nony, R. Boisgard, and J. P. Aime, J. Appl. Phys. **91**, 2537 (2002).

<sup>10</sup>M. Gauthier and M. Tsukada, Phys. Rev. Lett. **85**, 5348 (2000).

<sup>11</sup>C. J. Chen, *Introduction to Scanning Tunneling Microscopy* (Oxford University Press, New York, 1993).

<sup>12</sup>D. Sarid, *Scanning Force Microscopy with Application to Electric, Magnetic and Atomic Forces* (Oxford University Press, New York, 1994).

<sup>13</sup>J. P. Cleveland, B. Anczykowski, A. E. Schmid, and V. B. Elings, Appl. Phys. Lett. **72**, 2613 (1998).